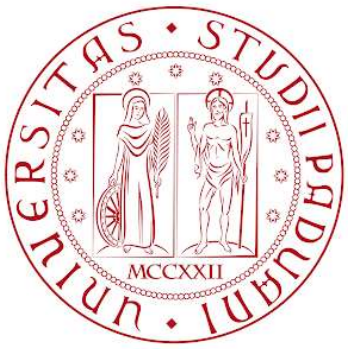

UNIVERSITÀ DEGLI STUDI DI PADOVA

Dipartimento di Ingegneria Industriale

Corso di Laurea Magistrale in Ingegneria dei Materiali

Tesi di Laurea

STUDY ON TRANSVERSE CRACKING IN AERO - ENGINE GRADE POLYMER COMPOSITE UNDER QUASI-STATIC LOADING

Relatore: Prof. Alessandro Martucci

Correlatore: Prof. Patrik Fernberg

Laureanda: Alessia Cardin

Matricola: 2044625

ANNO ACCADEMICO 2022 - 2023

The research project "*Study on transverse cracking in aero-engine grade polymer composite under quasi-static loading*" was conducted during my Erasmus traineeship at Luleå University of Technology (Sweden) within the Department of Engineering Sciences and Mathematics, Division of Material Science, during the second semester of the academic year 2022/2023. I wish to express my sincere gratitude to my supervisors, Prof. Patrik Fernberg and Prof. Roberts Joffe, along with the assistance of Dr. Vivek Richards Pakkam Gabriel. I deeply value their guidance and support, and I'm grateful for the chance to be a member of their research group.

Abstract

This work aims to contribute to the development of a damage prediction model for cross-ply laminates subjected to realistic use conditions of commercial aero-engine composite materials, including thermal cycling, isothermal aging and quasi-static load. The implementation of high-temperature polymer composites in aero-engines offers significant weight reduction, leading to reduced fuel consumption and environmental impact. The development of a damage prediction model is crucial to analyze the material's behavior avoiding the need for expensive and time-consuming tests under various conditions.

In this study, a composite laminate with a cross-ply configuration was utilized, and samples were subjected to isothermal cycling and aging at 150 °C, followed by quasi-static loading to investigate the evolution and behavior of intralaminar cracks, in terms of crack density. The crack density was then modeled using a statistical approach based on the Weibull distribution. This model enables the prediction of crack density evolution in the 90° layers of the cross-ply during quasi-static loading under different conditions, including as-built, cycled, and aged materials at both room temperature and elevated temperature of 150°C.

Experimental data obtained from quasi-static loading, degradation of the longitudinal elastic modulus after each load stage, and microscopic analysis of the microstructure of the cross-ply sample edges contributed to the development of the damage prediction model. By integrating these findings, a comprehensive understanding of the material's damage evolution and its corresponding mechanical response can be achieved, facilitating more accurate predictions of the life and performance of fiber-reinforced composite materials in aero-engine applications.

Contents

1 Introduction

The utilization of fiber reinforced polymer composite materials in various industries has experienced significant growth over the past decades due to the composite material's exceptional mechanical properties and lightweight nature. In particular, composite materials have found extensive applications in the aerospace industry, where their high strength-to-weight ratio, stiffness and corrosion resistance make them ideal for guarantee the performance and efficiency of aerospace structures [1]. However, ensuring the long-term reliability and life of composite materials in demanding environments remains a critical challenge.

Studies have shown that long term exposure to elevated temperatures can induce irreversible changes in the morphology, leading to a reduction of the performance. Additionally, cyclic variations between high and low temperatures, known as thermal cycling, can result in micro-damage accumulation and fatigue effect [2].

Among the various damage mechanisms, the initiation and propagation of transverse cracks in plies with fibers oriented in off-axis direction to the loading direction stands out as a predominant mode [3]. Transverse cracks propagate within the material parallel to the fibers direction, compromising its strength and initiating the delamination.

Therefore, understanding the initiation and propagation of this type of damage is critical for predicting the life of the material and for ensuring the safe and reliable operation of aero-engine systems.

However, testing and studying the life of these materials under different application conditions is resource-intensive and time-prohibitive. To address these challenges, developing a prediction model to supplement physical testing is beneficial in predicting the material's behavior [3]. By combining experimental techniques with statistical analysis, such as the Weibull distribution model, it is possible to understand the damage mechanisms and the transverse cracking behavior in aero-engine grade polymer composites.

1.1 Aim and Objectives

In this study, the primary aim is to investigate the thermo-mechanical behavior of aerospace grade composite material under conditions corresponding to realistic operation temperatures for certain aero-engine components. Certain components are operating at elevated temperatures ranging between around 150 °C to potentially 200 °C. These elevated temperature subject the material to significant thermal and mechanical stresses.

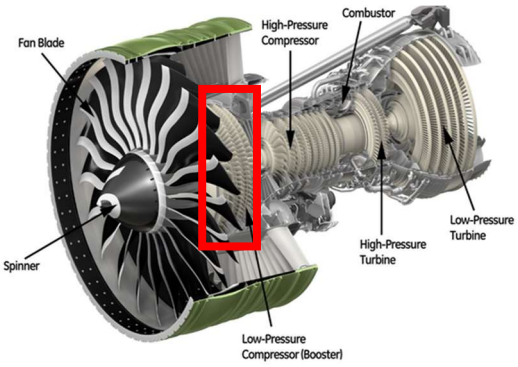

Fig. 1 Turbofan commercial aero-engine

This thesis aims to provide an understanding of the behavior of the specific composite material under simulated operating conditions of aero-engines. The physical characterization, tensile testing, and development of a crack density prediction model contribute to a better understanding of the material's structural integrity and thermal-mechanical performance.

A number of sub-studies were performed with the aim to contribute to the overall objective. In the first place, a physical characterization of the material was performed, investigating in detail with an optical microscope the microstructure of the composite before and after thermal treatments, as well as before and after each loading stages. This includes analyzing the evolution of the material's microstructure, identifying any changes in crack density, and assessing the overall damage state. The characterization provide valuable insights into the material's response to thermal treatments and mechanical loading.

Quasi-static tensile tests were conducted using different maximum strain levels at both room temperature and elevated temperature (150 °C). The aim of these tests is to induce damage and evaluate the material's mechanical response under various loading conditions, including its stress-strain behavior, elastic properties, and failure modes. The results were carefully analyzed to understand the material's mechanical properties and its ability to withstand tensile loads at different temperatures.

Furthermore, the material's behavior and response specifically under elevated temperature conditions were determined. This involves investigating the effects of thermal cycling and thermal aging separately on the material's mechanical performance.

The goal is to understand the influence of these factors on the material's strength, stiffness, and crack density evolution. By studying the material's behavior at elevated temperatures, particularly within the aero-engine operating range, the thesis aims to assess its suitability for high-temperature applications.

Finally a prediction model for intralaminar crack density specifically for cross-ply specimens was developed based on the experimental results. This involves utilizing statistical analysis techniques, particularly the Weibull model, to establish a relationship between applied stresses, environmental conditions, and the resulting crack density. The model was developed using the experimental data obtained from the physical characterization and tensile testing.
It serves as a tool for estimating and predicting the crack density in the composite material under various conditions, including elevated temperature as-built specimens, thermal cycled specimens, and iso-thermal aged specimens.

1.2 Theoretical background

1.2.1 Composite laminates

Composite materials are heterogeneous materials composed of two or more constituents with distinct properties, combined to create a final product with desired mechanical, thermal, or electrical characteristics. They are frequently employed as replacement of metals, offering several advantages such as reduced weight due to the low density of their constituents, a high strength-to-weight ratio and corrosion resistance.
Long fiber reinforced polymer composites, including carbon fiber, glass or aramid fiber, reinforced in thermoset resin like epoxy, bismaleimide or polyimide, are particularly favored for high temperature applications. These composites exhibit exceptional mechanical properties, thermal stability and resistance to degradation, making them suitable for demanding environment where traditional metals may not perform optimally.

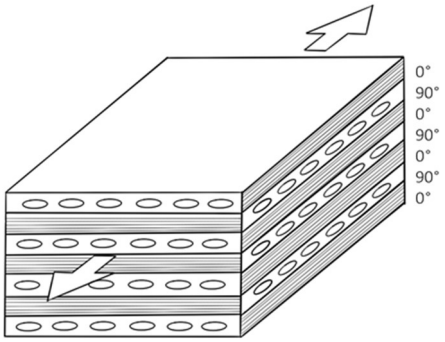

Fig. 2 Cross-ply laminate configuration

In the context of this study, a carbon fiber-reinforced polymer (CFRP) cross-ply laminate is utilized to investigate the material's behavior under realistic operating conditions. The

laminate consists of multiple layers of carbon fiber embedded in a matrix made of a high-temperature resistant polymer with a high glass transition temperature.
Carbon fibers are renowned for their exceptional mechanical properties, such as high strength, stiffness, and low weight. For instance, CFRP exhibits a minimum yield strength of 550 MPa, while its density is only one-fifth that of steel and three-fifths of aluminum-based alloys [4].
One significant advantage of polymer matrix composites (PMC) is their high specific strength and specific modulus. For instance, compared to aluminum-based alloys, CF-reinforced thermosetting resin composites offer significantly lower density along with three times higher tensile strength and twice the elastic modulus [5].

The choice of a heat-resistant polymer matrix is essential in composite materials to ensure their ability to withstand elevated temperatures while maintaining structural integrity and performance. A key characteristic of the selected polymer matrix is its high glass transition temperature. The glass transition temperature refers to the temperature at which the polymer transitions from a rigid glassy state to a softer rubbery state. A high glass transition temperature indicates the polymer's resistance to deformation and its capacity to retain structural properties even at elevated temperatures. This property is particularly important in applications where thermal stability is crucial. By incorporating a polymer matrix with a high glass transition temperature, the composite material can withstand challenging thermal conditions, ensuring long-term durability and preserving its mechanical properties.

Epoxy-based resins reinforced with carbon, glass, or aramid fibers have been widely used in composite materials but the focus now is on expanding their application to high-temperature environments, such as aero-engine components, where they are subjected to elevated temperatures and demanding conditions. The development of high-temperature polymer composites is categorized into two groups based on their service temperature ranges. The first group includes polymer-matrix systems with service temperatures ranging from 135-250 °C, including bismaleimides, cyanate esters and aromatic thermoplastics. The second group consists of polymer-matrix systems with service temperatures ranging from 250-350 °C, primarily composed of polyimides with high glass transition temperatures. Improvements in these resin systems result in composites with high mechanical properties but reduced weight loss and matrix cracking, leading to enhanced long-term performance and higher service temperatures.
Bismaleimides offer a highly cross-linked network with high glass transition temperature, good thermal stability, fire resistance, and low moisture absorption. Cyanate esters, although having lower thermal ratings than bismaleimides, exhibit superior dielectric loss properties and low moisture absorption, making them suitable for specialized applications. Bismaleimide composites have been successfully used for primary aircraft structures, rated for temperatures around 180 °C, while cyanate ester resins find applications in areas such as radomes, antennae covers, and stealth composites, offering good toughness comparable to toughened epoxies [10].

1.2.2 Intralaminar cracks

The first damage mechanism observed in composite laminates under tensile loading are the intralaminar cracks in the layers oriented transversely to the load direction, typically the 90° layers.
These cracks run parallel to the fiber direction and cover the entire thickness and width of the ply. They significantly alter the elastic properties of the laminate and can initiate other forms of damage, such as local delamination [7].
Transverse cracking occurs because strength of the composites are lower in the transverse direction compared to the longitudinal direction [8].
The development of intralaminar cracks can be divided in two phases: initiation and propagation.
The initiation stage occurs at individual fiber/matrix interfaces, involving the formation of cracks or debonding, followed by the coalescence of these small damage entities into a larger crack-like flaw. Once the flaw reaches a critical size, it grows unstably in the ply thickness direction before being arrested at the interface between plies. The transverse stress required to reach this critical size is known as the initiation strength [7].
Propagation of the flaw along the fibers requires a certain energy release rate (ERR), which depends on the ply stress and the size of the flaw. The ERR increases with the size of the flaw, and if it reaches the critical value (fracture toughness) before being arrested at the interface, propagation occurs. The stress necessary for crack propagation along fibers, referred to as propagation strength, decreases with increasing size of the damage entity.

1.2.3 Weibull model of intralaminar cracking

The 90-ply of the composite laminate is considered as consisting of a chain of independent elements of a length l_{ref}. The failure stress of different elements along the transverse direction of the ply varies.
In this study, the failure stress of each element within a 90-ply composite along the transverse direction is considered to follow a Weibull distribution [7]. The Weibull distribution is employed in the analysis of failure behavior in composite materials and it is characterized by two parameters: the shape parameter m and the scale parameter σ_0.
The determination of the Weibull parameters involves experimental investigation, particularly through the examination of crack density growth versus applied strain data.
The probability of failure P_f is the expected fraction of elements that have failed during the stress increasing from 0 to σ_T, so the probability of failure at a specific stress level, σ_T, can be predicted using the following expression:

$$P_f = 1 - \exp\left[-\left(\frac{\sigma_T}{\sigma_0}\right)^m\right] \tag{1.1}$$

where σ_T is the applied thermo-mechanical transverse stress in 90 layer and σ_0 and m are the Weibull scale and shape parameters respectively obtained from experimental data. This model accounts for the probabilistic nature of failure, taking into account the variability of failure stress within the composite due to its inhomogeneity.

In practical situations where a ply contains cracks, the transverse stress distribution is non-uniform. However, by utilizing the Classical Laminate Theory (CLT) transverse stress, which includes both mechanical and thermal residual stresses, the analysis becomes more manageable [7]. The CLT transverse stress corresponds to the load applied to the undamaged laminate, simplifying the calculation of failure probabilities.
The element length is defined as equal to the thickness of the 90-ply composite t_k. As crack density approaches an asymptotic value, with crack spacing approximately equal to t_k, the maximum crack density, can be estimated as the reciprocal of t_k. Thus, φ_{max} represents the upper limit of crack density within the composite laminate.

$$\varphi_{max} = \frac{1}{t_k} \tag{1.2}$$

The experimental probability of failure at a given stress level σ_T, can be calculated by dividing the crack density at that stress level by the maximum crack density.

2 Experimental methods

This chapter focuses on the experimental methodology employed to study the damage behavior of the material under various conditions. It includes a description of the employed material, the experimental configuration and testing and modeling procedure.

2.1 Material and specimen configuration

In this study, a carbon fiber reinforced high temperature thermosetting polymer plate with a cross-ply laminate configuration was utilized. Specifically, the cross-ply plate consisted of three 90° layers and four 0° layers arranged in a [0/90/0/90/0/90/0] lay-up, with a nominal thickness of 1.15 mm.

Fig. 3 Microstructure of cross-ply sample edge

The plate was manufactured using resin transfer molding technique. The manufactured plate was then sectioned into rectangular specimens with a nominal length of approximately 170 mm and a width of 15 mm. Successively, the longitudinal borders of each specimen were carefully grinded and polished in order to have a clear surface for the edge damage investigation in optical microscope. A 50 mm region was selected as the analyzed area for each sample since the focus of the study was on crack density, and it was not necessary to examine the entire length of the specimen.
The as-built specimens underwent a primary microstructure analysis in both of the edges using an optical microscope to inspect for surface defects resulting from manufacturing, cutting, and grinding processes that may impact sample performance during testing. Minor defects, such as small scratches and few voids are identified and their effect on the stiffness was successively studied since they have the potential to evolve into cracks over time. Then, major defects, such as cracks that extend beyond half of the thread region, were reported and acknowledged as compromising the mechanical performance, as they have the potential to propagate and initiate larger cracks.

A random subset of specimens was chosen for testing, 12 in total; and dimensional and stiffness data of the specimens before any treatment and test were measured.
Further information about the transverse modulus, Poisson ratio, fibers volume fraction and thermal expansion coefficient were obtained from a previous study of the same material in UD configuration [9]. These data were used successively to calculate the transverse stress state in the 90 layers of the cross-ply samples through the classical lamination theory (CLT) using the software LAP.

2.2 Sample conditioning

Previous studies [9] revealed that the material undergoes significant changes when subjected to mechanical cyclic loading at elevated temperature, material experiences both thermal cycling and thermal aging effects. This study aims to explore these effects individually and examine their distinct influences on the thermo-mechanical performance of the material. To achieve this, three sets of specimens were prepared, each set exposed to different thermal conditions: as-built specimens representing the pristine state after manufacturing, thermally-cycled specimens undergoing 15 cycles at a temperature of 150°C, and isothermally aged specimens subjected to a 1000-hours exposure to a temperature of 150°C with air.
.
The as-built revealed the presence of transverse cracks, which were attributed to the stress experienced during the cooling process after manufacturing. In fact, the cooling process from the curing temperature to room temperature introduces defects and residual thermal stresses within the material.

The thermally-cycled specimens were subjected to a series of repetitive thermal cycles. These cycles involved rapid heating the specimens to a temperature of 150°C in an ambient air environment, followed by a rapid cooling to room temperature (21°C). Each heating stage lasts 25 minutes, while the subsequent cooling stages last for 15 minutes. The thermal cycling procedure was executed according to the provided scheme showed in fig.4.

Throughout the thermal cycling process, the number of cracks within the specimens was quantified at specific intervals, such as after 3, 7, 10, and 15 cycles. Additionally, any weight loss incurred by the specimens was monitored, providing insights into potential degradation.

Furthermore, aging in different set of specimens was conducted within an ambient air environment, where the specimens were exposed to a temperature of 150 °C over a continuous duration of 1000 hours. Weight loss measurements were recorded before and after the aging process, and crack counting was performed to assess any changes in the crack density.

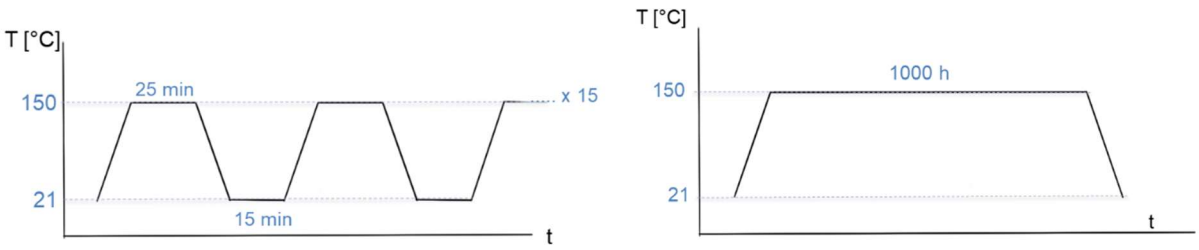

Fig. 4 Thermal cycling and aging procedure scheme

The conditioned specimens were subjected to quasi-static tensile tests. Each of the three sets (as built, cycled and aged) consists of four specimens, resulting in a total of twelve specimens. Within each set, two specimens were tested at room temperature, while the remaining two specimens were tested at elevated temperature. The table below is a schematic representation of the planned test configuration for each specimen, with the specimens identified by numbers.

Tab. 1 Sample ID for as-built, cycled and aged and quasi-static test temperature

Type	Sample ID number	Quasi-static Tensile Test Temperature
As-built	5	Room T
	39	
	19	Elevated T (150 °C)
	36	
Cycled	33	Room T
	40	
	3	Elevated T (150 °C)
	13	
Aged	2	Room T
	9	
	7	Elevated T (150 °C)
	34	

2.3 Quasi-static tensile tests

Quasi-static tensile tests were conducted at various mechanical strain levels, ranging from 0.3% to 0.9%, with incremental steps of 0.1% (e.g., 0.3%, 0.4%, 0.5%, and so on). In some specimens, additional tests are performed at strain levels of 0.75% and 0.85% to gather more data. The displacement rate was set at 2 mm/min for both loading and unloading. Axial strain after each loading step was measured using a dynamic extensometer placed in the 50 mm portion of the sample.

The aim of the quasi-static tensile tests is to induce damage in the material and characterize it through optical investigation. The number of cracks created after each loading step was counted, providing data for calculating the crack density. Additionally, the longitudinal elastic modulus was determined before and after each damage stage to assess the degradation of the material's elastic properties with increasing strain.

Initially, two specimens for each set underwent tensile tests at room temperature to collect data on the material behavior under different maximum strain levels. This step allows to establish a baseline for the comparison between the behavior of as built specimens and those subjected to the preliminary conditioning treatments and to develop a prediction model specifically tailored.
Subsequently, the remaining two specimens for each set underwent the same tensile tests at elevated temperature of 150 °C, allowing for an investigation of the material's response under realistic conditions similar to those experienced in the compressor of an aeroengine.
All the tests were performed using an Instron ElectroPuls E10000 Linear-Torsion machine with a 10 kN load cell, for the elevated temperature an Instron 3119-605 environmental chamber was used.

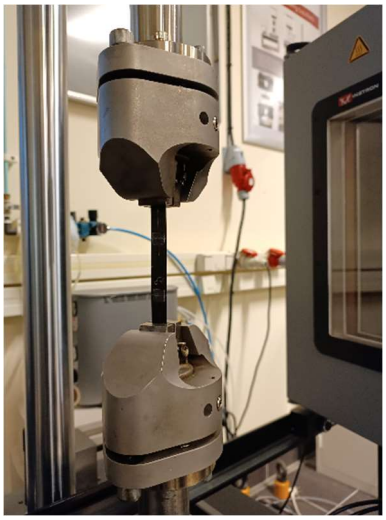

Fig. 5 Sample mounted on quasi-static test machine

Stiffness measurements of the sample were made before and after each stage to check the longitudinal elastic modulus E_x evolution during testing. These values are obtained from quasi-static tests performed up to 0.15 %. This low strain level was employed to avoid additional damage to the material, as the primary objective is to measure the elastic modulus rather than induce extensive damage.
Data corresponding to the axial strain interval between 0.12 % - 0.05 % of the unloading ramp was used in the post-processing stage for the calculation. This interval was selected in order to avoid the fluctuation in the measurements arising at the initial and final data of each ramp.

As the testing progressed, the load and strain levels gradually increased. However, when the strain reached approximately 0.6%, the testing machine's load capacity of 10.000 Newton was nearly reached. To accommodate this, it was necessary to reduce the cross section of the

samples. Consequently, after reaching a strain of approximately 0.6%, each specimen underwent again a grinding and polishing process along one of the edges to reduce the cross section. Following, the cross sections were measured, and the number of cracks was counted to assess whether there were any disparities in crack density between the surface and bulk regions of the specimen. Specifically, to determine if the cracks exhibited tunneling behavior. By reducing the cross-section, the maximum load required to achieve the desired strain was effectively decreased.

2.4 Data collection and post processing

The cross-section of each specimen was calculated based on the average of three measurements of width and thickness.
The mechanical stress acting on the specimen at a given load was determined by dividing the applied load by the cross-sectional area.
In addition, strain data, which provides information about the deformation of the specimens during the tensile tests, was also collected. To capture this data, an extensometer with a length of 50 mm was carefully affixed to the specimens.
To determine the elastic modulus of the material before and after each damage step, stress-strain curves were plotted using the collected data. The longitudinal elastic modulus was calculated as the slope of the stress-strain curve within the strain interval of 0.12% - 0.05% of the unloading ramp.

Moreover, the extent of damage was examined for each specimen after every strain level. Upon removal from the testing machine, the specimens were subjected to detailed damage analysis under an optical microscope. Specifically, both edges of each specimen were inspected, with a focus on identifying and quantifying cracks in each 90° layer. These cracks were categorized into three distinct types for separate counting: cracks in the threads, cracks in the threads that spread in the bundles, and cracks in the bundles.
Cracks in the threads, as shown in fig.6 (a), primarily emerge during the early stages of the tests, as the threads represent the weakest portion of the layer. Since the fibers in this region are glass fibers with a smooth surface, their bond with the polymeric matrix is relatively weak.
Only cracks of sufficient size that traverse the entire thread zone were taken into account. In cases where two cracks occur within the same thread zone, they were counted as one, as they likely originate from a single crack branching on the surface.
Applying load, the cracks initially present in the threads begin to propagate and extend into the adjacent bundles, leading to the formation of individual cracks within both the threads and the bundles, as shown in fig.6 (b).
Finally, cracks in the bundles occur within the bundle zone, which consists of carbon fibers – matrix debonding, like in fig.6 (c).

Occasionally, instead of removing the specimens from the testing machine for crack counting, resin replicas were taken from the 50 mm region of interest along both edges. This approach saves considerable time, as the replicas can be analyzed at any convenient moment. The Struers' Repliset system was employed to create these replicas. A 50 mm straight line was

marked on a sheet of baking paper, which includes essential data such as the sample number, the corresponding edge, and the load stage. Subsequently, a strip of resin was applied along this marked line to ensure capturing the desired length. Prior to applying the resin to the edges of the sample, a 700 N load was applied to enhance crack opening and facilitate easier identification of cracks in the replicas. The resin was left to cure for 8 minutes. Once removed, the replicas were examined under a light optical microscope using the same procedures as the actual specimens. The replicas exhibit sufficient quality for microstructural analysis.

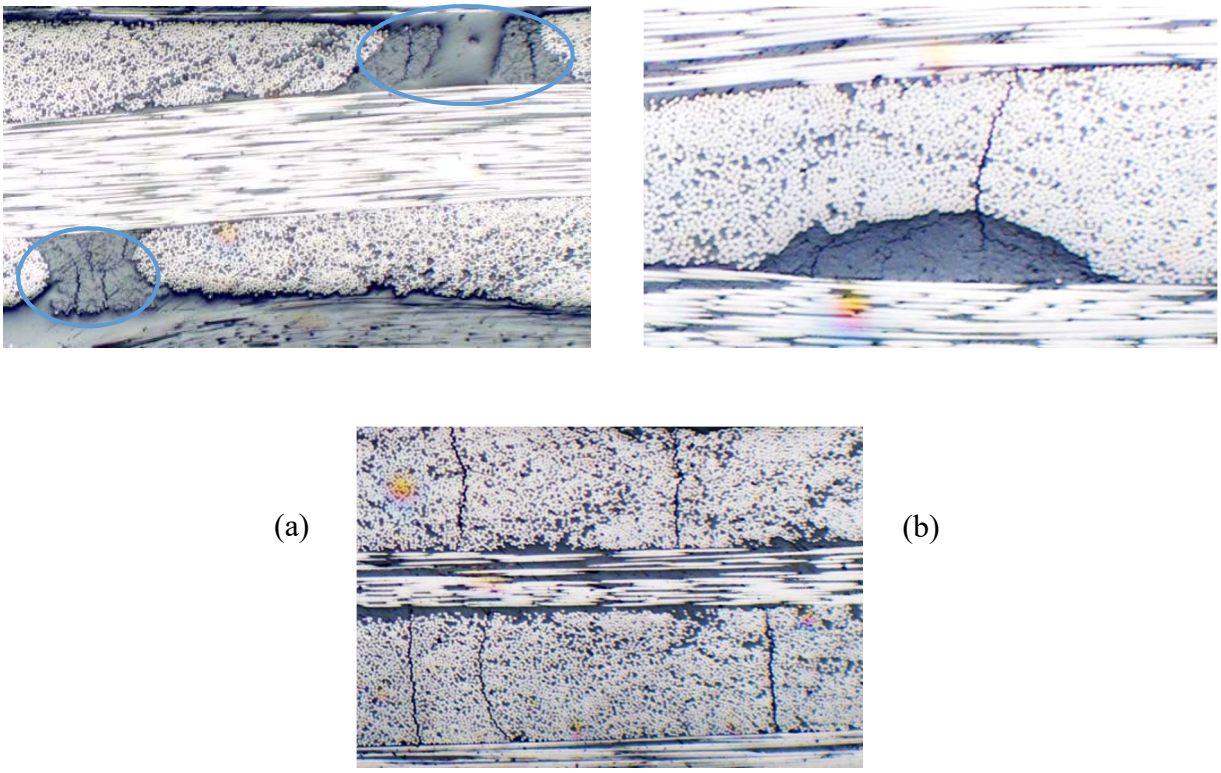

Fig. 6 Cracks in the 90 layer: (a) in threads, (b) from threads to bundle, (c) in the bundles

2.5 Crack density and Weibull model

The specimen, a composite with three 90-layers in the layup, offers a total of six visually observable 90-layer surfaces, three on each edge. For each of these surface layers, cracks were counted distinguishing them into the three categories: cracks in the threads, cracks in the bundles and cracks both in the thread and in the bundle. To determine the overall crack density of the single specimen, the average number of cracks in the 90-layer is first calculated. This is done by dividing the sum of the total number of cracks observed in all six 90-layers by six. Subsequently, this average is further divided by the length of the observed zone of the specimen, which is 50 mm. Consequently, the overall crack density was expressed as cracks per millimeter (cracks/mm).

Finally, the probability of failure was determined by calculating the ratio between the crack density and the maximum crack density. The maximum crack density was derived by taking the reciprocal of the thickness of the 90-layer region, as explained in section 1.2.3.

The first step to develop a crack density model was to determine the Weibull parameters, namely the shape and scale parameters. They were obtained by plotting on logarithmic scale the thermo-mechanical transverse stress in 90-layers against the logarithm of the probability of failure for each specimen, as reported in the formula below.

$$ln\big(-ln\big(1-P_f\big)\big) = m \cdot ln(\sigma_T) - m \cdot ln(\sigma_0) \tag{1.3}$$

From the linear data points of the logarithmic graph, shape and scale parameters were obtained. Parameters of all the specimens were obtained as a comparison, but for the prediction model only the parameters of the reference condition as-built tested at room temperature was used in the following formula (prediction of probability of failure).

$$P_f = 1 - \exp\left[-\left(\frac{\sigma_T}{\sigma_0}\right)^m\right] \tag{1.1}$$

A comparison was made between the experimental probability of failure and the predicted value, the results are presented in the subsequent chapter. However, it was empirically observed that the parameters require correction to accommodate different scenarios, such as as-built specimens tested at elevated temperatures, cycled and aged specimens. Therefore, in this study, a procedure is implemented to adapt the prediction model for these various cases through parameters correction. This correction procedure was made through some corrective factors that are function of tested temperature and heat treatment conditions. By applying the corrected parameters, the prediction model can provide more accurate estimations of the probability of failure for the different scenarios encountered in the study. In the upcoming chapter, the results of this adapted prediction model are presented and discussed, highlighting the effectiveness of the correction procedure.

3 Results and Discussion

This chapter presents and analyzes the experimental findings regarding the evolution of damage in terms of crack density and the degradation of the elastic modulus observed during the quasi-static tensile tests conducted on the three sets of specimens.
Additionally, the effects of thermal aging, thermal cycling and the elevated temperature on the material are examined.
Finally, the calculation of Weibull parameters and the implementation of a predictive model to estimate the progression of damage are discussed.

3.1 As-built material characterization

Firstly, an initial optical inspection was performed on each specimen to analyze its microstructure before any thermal treatment or testing and to quantify the initial damage created during the manufacturing process. Also an initial quasi static tensile test at 0.15% strain was performed for each specimen to determine the initial elastic modulus.
The cracks observed prior to testing were primarily located only in the threads and not in the bundles. This aligns with expectations since the threads represent the weakest region of the layers due to the presence of glass fibers, resulting in a weaker bond with the matrix.
Also few voids were identified in the 90-layer. Voids were not quantified, neither by size nor count. However, it is expected that they may serve as initiation points for crack formation during subsequent tensile tests or thermal treatments.

3.2 Thermal cycling

Following the thermal cycling procedure described in paragraph 3.1, four specimens (33, 40, 3, 13) underwent thermal cycling at 150 °C for 15 cycles and then its effect was investigated. The evolution of crack density after 3, 7, 10, and 15 cycles is represented in the following graph in Fig.7.
From the graph in Fig.7 it is evident that there is an increase in crack density as the number of cycle increases. It should be noted that these cracks were observed in the threads and they did not spread to the bundles, so the increase in crack density is primarily attributed to the growth and opening of pre-existing threads cracks that were previously too small or weakly visible to be counted.

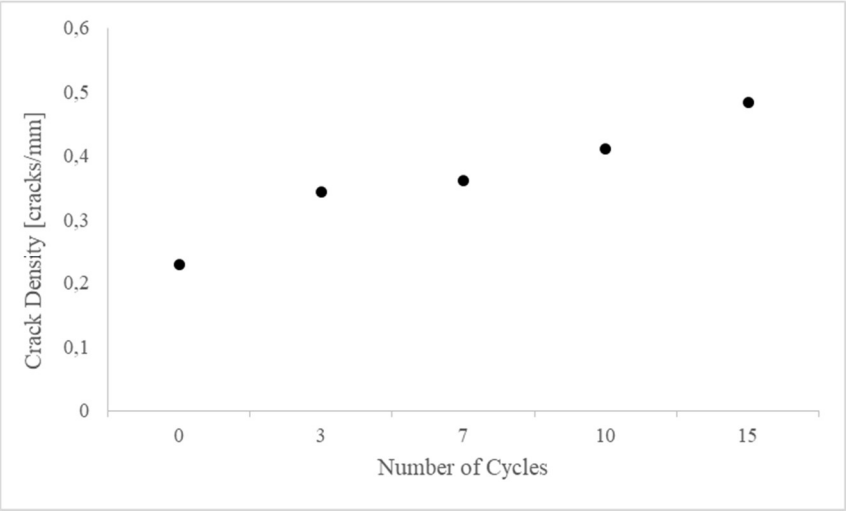

Fig. 7 Crack density vs Number of thermal cycles between RT and 150°C

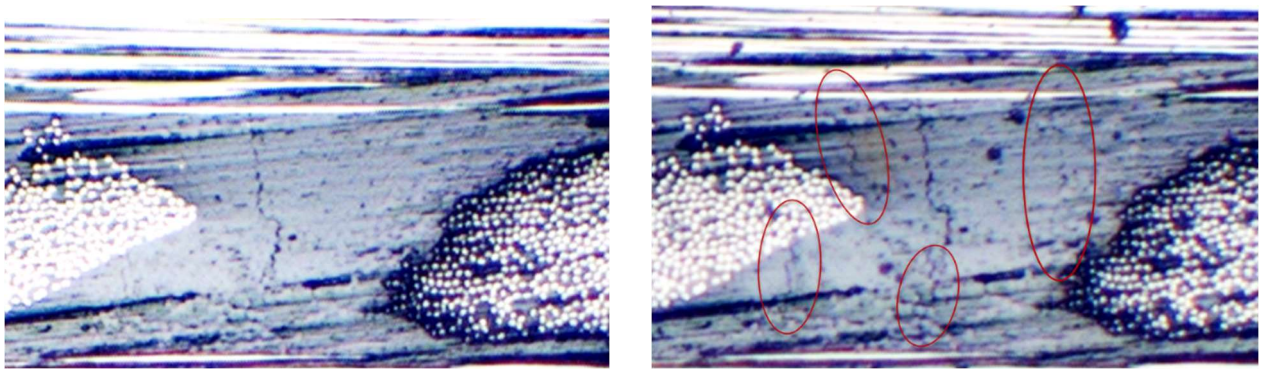

(a) (b)

Fig. 8 Cracks in the threads (a) before and (b) after 15 cycles

The cracks in the threads after 15 cycles (Fig.8(b)) were already present even before the cycling process (Fig.8(a)). However, before cycling these cracks are not well visible since they are very small, but they opened and become more pronounced during the cycling stage. This suggests that the predominant effect, in this case, was the matrix shrinkage that caused the debonding of the weaker bond between the matrix and glass fibers. In fact, the repeated thermal expansion and contraction between the carbon fibers and the polymer matrix can lead to the development of interfacial stresses. Over time, these interfacial stresses can result in the debonding and sliding of the fibers within the matrix, compromising the load transfer efficiency, contributing to the decrease in the elastic modulus and the opening of already existing cracks and the formation of new cracks.

However, it is important to note that even though from the optical investigation the damage appeared to be relatively mild, characterized by a small number of cracks confined to the threads, it is still expected it to contribute to the degradation of mechanical properties. The

impact of these cracks on the overall material performance is further examined by analyzing the results of the tensile tests in the upcoming chapter.
In fact, it can be assumed that 15 cycles are not sufficient to cause significant fatigue related degradation of the microstructure, which can be observed instead at higher cycle numbers.
In this study, the thermal cycling was limited to a total of 15 cycles due to time constraints. Future studies with a greater number of cycles could provide additional insights into the long-term behavior and durability of the material under thermal fatigue cycling conditions.

Also weight loss was monitored during the thermal cycling stage. The graph below clearly indicates a reduction in the total weight of two specimens, amounting to 23.6 milligrams. The majority of this weight loss appears to occur during the early stage of the treatment, specifically within the first 3-7 cycles.
One potential cause of this weight loss can be attributed to the loss of water and other dissolved gasses. This hypothesis is supported by the subsequent weight measurement conducted three days after the treatment's end, which showed an increase in weight from 8.575 g (immediately after 15 cycles) to 8.582 g. This weight gain can be attributed to the absorption of moisture from the surrounding air during the three-day period.

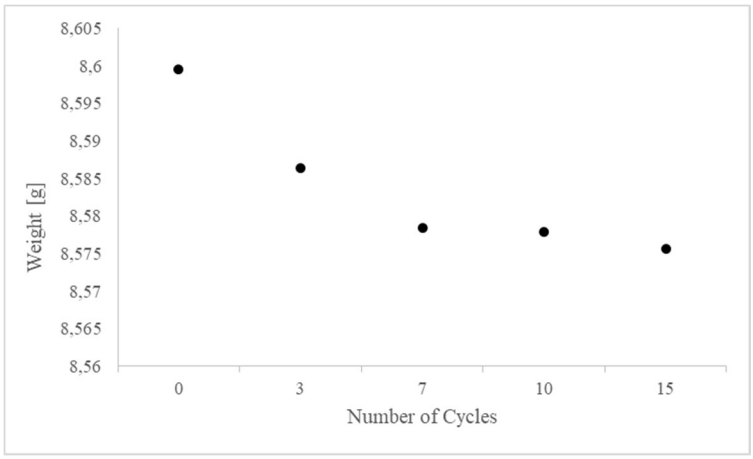

Fig. 9 Weight loss during isothermal cycling

Furthermore, there is a possibility that the weight loss is not solely due to the evaporation of water, but also to the degradation of the polymeric matrix, evaporation of volatile components or potential oxidation processes.

3.3 Thermal aging

Following the thermal aging procedure described in paragraph 3.1, four specimens (2, 9, 7, 34) underwent isothermal aging at 150 °C for 1000 hours with air and then its effect was investigated.
To analyze the distinct impacts of thermal cycling and exposure to high temperatures, a comparative investigation was carried out. In the thermal cycling process explained before the specimens are subjected to 15 cycles, each lasting 25 minutes at 150 °C, resulting in a total duration of 6 hours and 15 minutes of high temperature exposure.
So during the thermal aging treatment, two specimens were extracted from the oven after the same duration of 6 hours and 15 minutes to evaluate the evolution of crack density and compare it with the cycled specimens data.
To mitigate potential effects of thermal shock, a controlled cooling process was implemented. With this procedure initially, the oven is switched off, and the specimens were left inside with the door closed for one hour. Subsequently, the door was opened, and an additional 30 minutes was allowed for the specimens to acclimate. Then, the samples were removed and allowed to cool down to ambient temperature for an additional 15 minutes before further analysis.
The same cooling procedure was performed at the end of the aging process after 1000 hours.
The graph in Fig.10 below displays the crack density data recorded before and after the 6 hours and 15 minutes aging period, compared with crack density data of the cycled specimens.

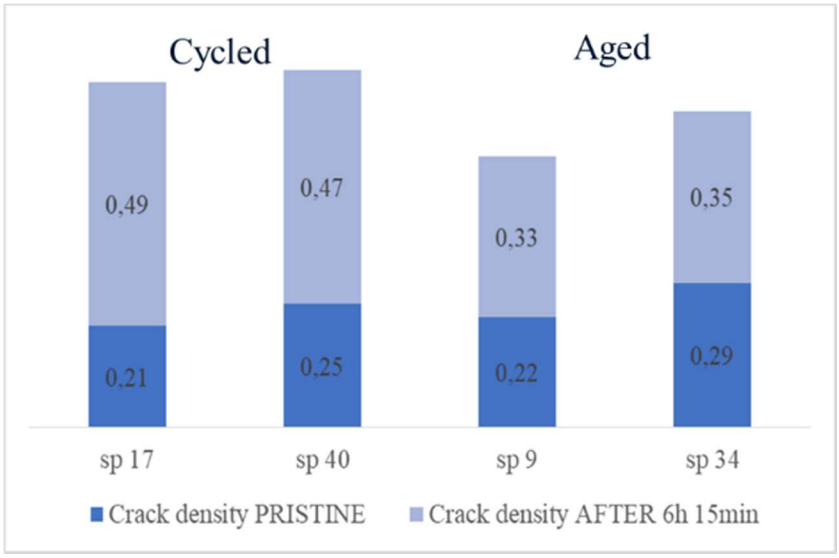

Fig. 10 Comparison crack density before and after 15 cycled and before and after 6h and 15min aging

It should be noted that also in this case for the aged specimens, the increase in the number of cracks can be attributed more to the opening of pre-existing cracks in the threads rather than the formation of new cracks.
It becomes apparent that the crack density of the aged specimens, which initially showed a similar initial value to the cycled specimens at approximately 0.2 cracks/mm, exhibits a slightly lower increase compared to the specimens subjected to thermal cycling. This finding

suggests that the effect on the material's structural integrity is not solely attributed to the exposure to a temperature of 150 °C but also to the continuous and rapid variation between high and room temperatures experienced during the thermal cycling process has a remarkable effect. Thus, 15 thermal cycles induce more damage than the exposure at elevated temperature for the same total exposure time of 6 hours and 15 minutes.
The continuous expansion and contraction, along with the mismatch in thermal expansion coefficients between the matrix and fibers, generate internal stresses and strains within the material. These factors can contribute to both the opening of pre-existing cracks and the initiation and propagation of new cracks.
The further average crack density of the four aged specimens after 1000 hours of exposure at 150 °C is reported below.

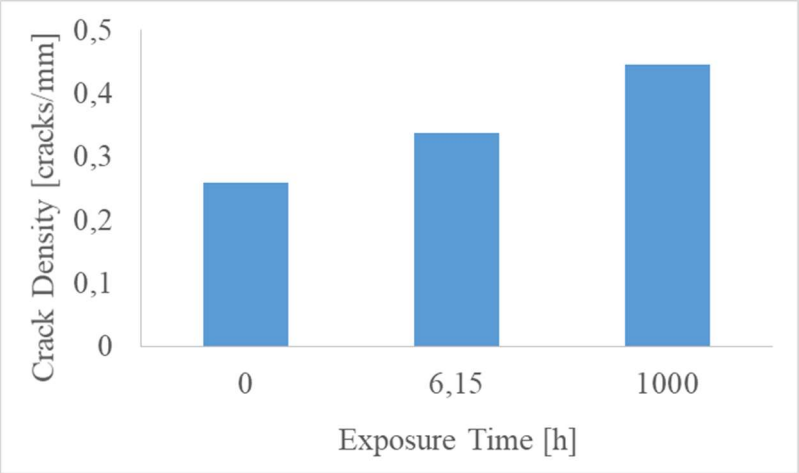

Fig. 11 Crack density evolution during aging

From Fig.11 it is evident that the crack density significantly increased after 1000 hours of aging, nearly doubling from the initial value, before the treatment, of approximately 0.2 cracks/mm to around 0.4 cracks/mm after the exposure.
It must be noticed that a substantial increase in crack density was already observed after 6 hours and 25 minutes of exposure. Specifically, there was a 68.3% increase in crack density during the initial 6 hours and 15 minutes, while the subsequent 1000 hours saw a 31.7% increase, suggesting that the effect of thermal aging becomes apparent in the early stages of high-temperature exposure.
However, it is important to note that the observations are based on a limited number of tested specimens, and further investigations are required to establish this trend more confidently.

As mentioned earlier, the increase in crack density primarily resulted from the opening of existing cracks in the threads. Nevertheless, after 1000 hours of aging, it was observed the formation of new cracks within the bundles as well. For instance, specimen number 7

exhibited 5 cracks in the bundles, while specimen number 9 displayed 2 cracks originating in the threads and spreading into the bundles.
These cracks in the bundles represent a more severe form of damage, indicating that prolonged exposure to high temperature of 150°C has a significant impact on the microstructure. This effect extends beyond the weaker region of the 90 layer and also affects the bundles, where the adhesion between the carbon fibers and matrix is stronger.

The average total weight of the four samples was measured prior to the treatment and it corresponds to 16.82 g; successively after 6 hours and 15 minutes decreases at 16.76 g and after 1000 hours of aging it corresponds to 16.78 g.
As expected, a decrease in weight is observed after 1000 hours of aging, which can be attributed to the same factors discussed earlier, including water loss, evaporation of volatile components, and oxidation and degradation of the matrix.
Interestingly, similar to the trend observed in the evolution of crack density, the most significant weight change occurs within the first 6 hours and 15 minutes of the aging process, rather than during the subsequent 1000 hours, where indeed a slightly increase is noticed, probably due to absorption of moisture or simply data scattering.

Following the analysis of the crack density and weight loss evolution after the 1000-hour exposure to 150 °C, it was expected that the longitudinal elastic modulus would decrease. However, comparing the initial elastic modulus before aging with the values measured after the treatment, an unexpected observation was made, shown in the table below: the elastic moduli of all four specimens actually increased slightly.

Tab. 2 Elastic modulus before and after 1000 h aging at 150°C

Sample Id Number	Stiffness [Gpa] Before Aging	Stiffness [Gpa] After Aging (1000h)
2	81,85	83,98
9	84,04	84,95
7	82,67	83,71
34	83,1	87,51

To justify this it can be assumed that there are more competing mechanisms during the thermal aging process, particularly in polymer matrices. While thermal aging typically leads to matrix degradation and a potential loss of mechanical properties, it is important to recognize that a long exposure at elevated temperatures can also activate additional reactions. One such reaction is the curing process, which is triggered by the elevated temperature and initiates the formation of new cross-links between molecules that were not fully reacted during the initial manufacturing process. As a result, the material experiences an increase in cross-linking density, leading to a stiffer and potentially more brittle structure.
However, it is important to note that the increase in the elastic modulus observed in this case does not necessarily imply an improvement in material cracking resistance. Instead, it could

have adverse effects on the overall mechanical behavior if the increase in stiffness is associated with embrittlement of matrix.
Such increased stiffness and brittleness can lead to a less favorable stress distribution within the material. Consequently, when subjected to mechanical stress, the aged specimens may experience a decreased crack resistance compared to their initial state. This phenomenon is further demonstrated and discussed in the subsequent section 4.4, where the crack density data during quasi-static tests are presented.

In conclusion of the investigation into the changes induced by the sample condition in the form of thermal cycling and thermal aging treatments, it can be observed that there is an increase in crack density but the increase is relatively minor, primarily attributed to the opening of pre-existing cracks rather than the formation of new ones. Similarly, the weight loss and alterations in the elastic modulus are not significantly pronounced. Consequently, a moderate reduction in mechanical performance is expected.

3.4 Quasi-static tensile tests at room temperature

After investigating the effects of sample conditioning through thermal treatment and characterizing the initial microstructure, quasi-static tensile tests were conducted at both room and elevated temperature of 150 °C. In this section, the focus is on the results obtained at room temperature. Two specimens for each type (as built, thermal cycled, and thermal aged) were tested: specimens 5 and 39 from as-built, 33 and 40 from cycling, and specimens 2 and 9 from aging.

The following graphs in Fig.12 show the evolution of crack density as a function of applied mechanical strain. Consistent with the theory of damage evolution, an increase in mechanical strain or thermo-mechanical transverse stress results in a significant increase in crack density. The graph of crack density versus the thermo-mechanical transverse stress in 90 layer has the same trend.
From Fig.12 it is evident that there are distinct differences among the data points for the as-built, cycled, and aged specimens. Notably, for the same applied mechanical strain, the crack density is slightly higher for the thermally cycled specimen compared to the as-built specimen, and even higher for the aged specimen. This indicates that the previous thermal treatments induced visible damage in the microstructure, resulting in a reduction of mechanical properties and a decrease in cracking resistance.

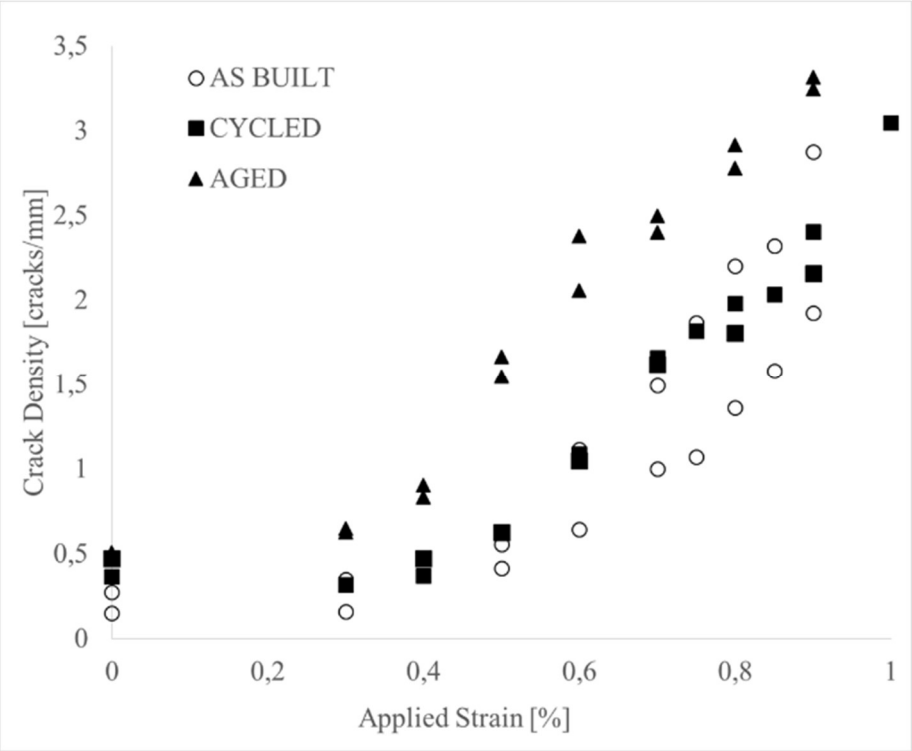

Fig. 12 Crack density evolution vs applied strain during quasi-static tests at room temperature

Moreover, it is evident that the aged specimens exhibit lower mechanical performance in terms of cracking resistance compared to the cycled specimens. This is expected, considering the more significant impact of 1000 hours of exposure at 150 °C compared to the relatively shorter duration of 6 hours and 15 minutes in the thermal cycling treatment; also because 15 cycles are not enough to induce considerable damage.

The elastic modulus was measured after every test, in order to track its degradation under different strain levels. It is expected that an increase in damage would result in a decrease in the modulus as the mechanical load increases. However, the observed degradation reported in Fig.13 does not follow a completely consistent trend in the sense that some values exceed the initial modulus. The variation is attributed experimental uncertainties originating e.g. from potential variations in extensometer alignment of and specimen after each strain level. In fact, after each test, both the extensometer and the specimens, or only the extensometer whenever replicas were taken, were removed for optical inspection, leading to potential misalignment and subsequent calculation discrepancies.

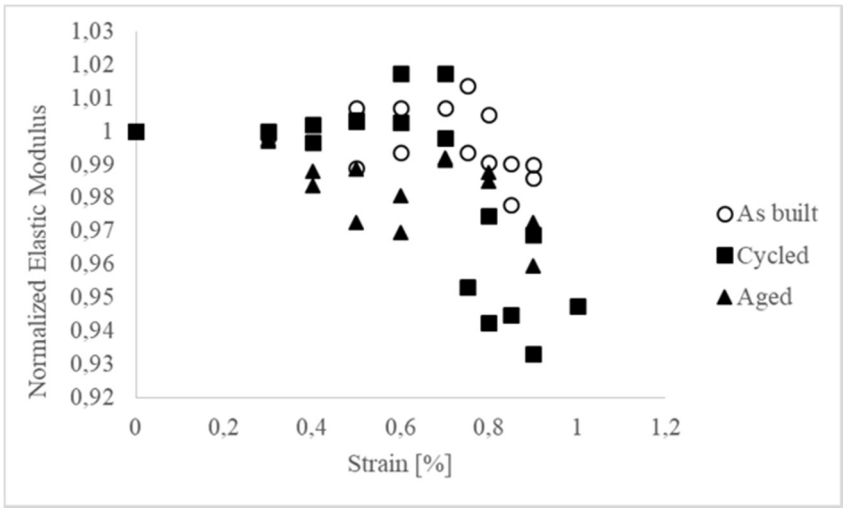

Fig. 13 Normalized elastic modulus evolution versus applied strain during quasi-static tests at room temperature

Despite these variations, these fluctuations are not so pronounced and the overall trend still indicates a decrease in the elastic modulus, with the final value lower than the initial value. Moreover, from the graph in Fig.13 it is evident that the overall data points of the conditioned specimens exhibit a slightly lower elastic modulus compared to the as-built specimens. Additionally, the percentage decrease from the initial to final values after quasi-static tests is, on average, 2.2% for the as-built specimens, 5.2% for the cycled specimens, and 4.4% for the aged specimens. These findings indicate that the thermal treatments have an effect on the elastic properties, resulting in a more pronounced degradation for the treated specimens. Contrary to expectations, the percentage decrease in the elastic modulus during the quasi-static tests for the aged specimens is lower than that of the cycled specimens. This can be attributed to the aforementioned calculation discrepancy or the increased brittleness of the aged material, which resists variations in the elastic modulus.

The damage observed in the specimens manifests as the formation and propagation of cracks, both originating from the threads and propagating into the bundles, as well as cracks exclusively within the bundles. As the strain level increases, this damage was accompanied by increasingly perceptible acoustic emissions. The following images (Fig.14) provide a comparison of the damage state in a portion of the 90-layer for the three specimen sets (as-built, cycled and aged) at the same strain level of 0.7%. It is evident that the number of cracks is higher in the cycled specimens compared to the as-built specimens, and even higher in the aged specimens.

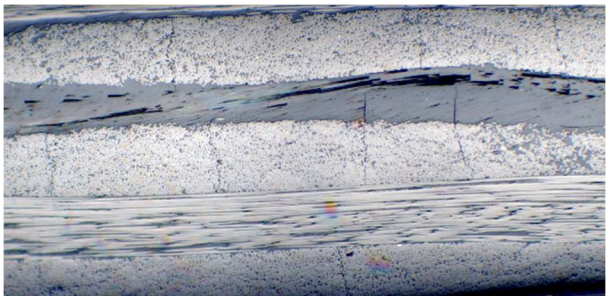

(a)

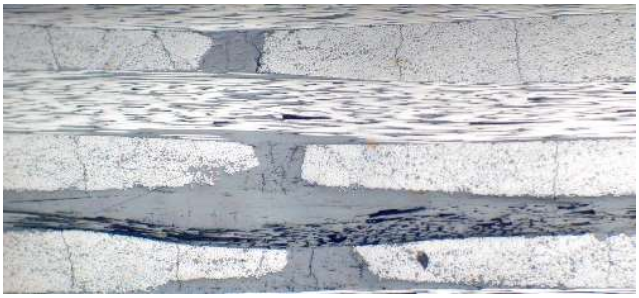

(b)

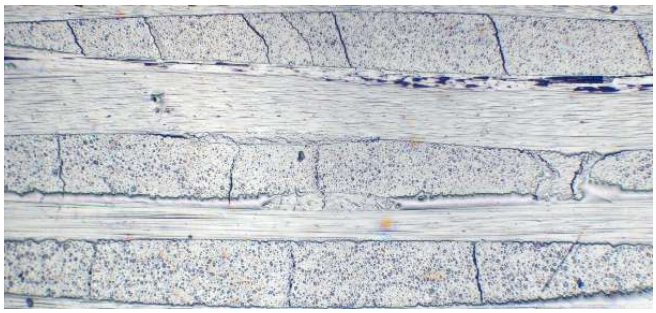

(c)

Fig. 14 90 layers cracks in (a) as-built, (b) cycled, (c) aged, after 0.7% strain quasi-static tests at room temperature

Furthermore, at approximately 0.6-0.7% strain, or even earlier in the aged samples, local delamination started to occur, coinciding with a visible drop in the elastic modulus on the graph. Delamination became more pronounced and prevalent in the aged specimens during the later stages of the test, at 0.9% strain, resulting in significant debonding between the layers. However, this phenomenon was not observed to the same extent in the other types of samples. This indicates that prolonged exposure to elevated temperatures (aging) induces more severe microstructural degradation in the material. This is shown in the following Fig.15.
Overall, these findings demonstrate that the thermal cycling and aging have an influence on the material's transverse cracking resistance.

All this data collected, particularly the crack densities, served as input in the next phase of developing a customized Weibull model for predicting damage in materials subjected to thermal cycling and aging.

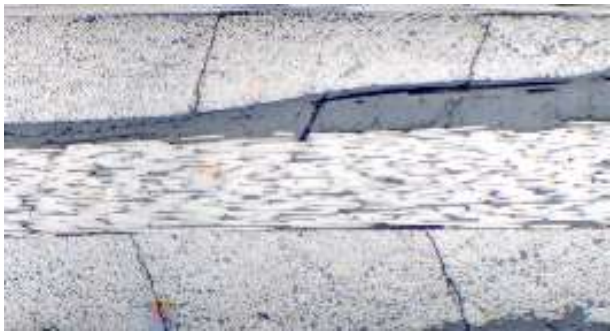

(a)

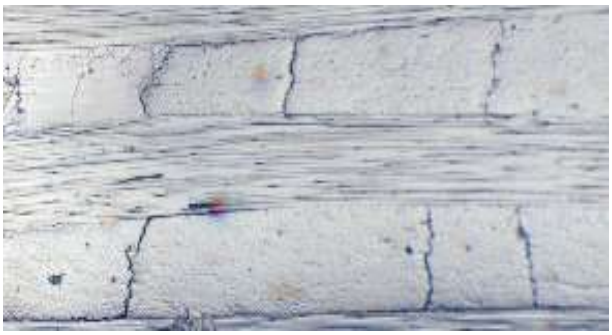

(b)

(c)

Fig. 15 Delamination in (a) as-built, (b) cycled, (c) aged, after 0.9% strain quasi-static tests at room temperature

3.5 Quasi-static tensile tests: comparison room and elevated temperature

After conducting the tests at room temperature, quasi-static tensile tests were performed at an elevated temperature of 150°C in a heating chamber, following the procedure explained in section 3.2. Two specimens of each type (as-built, thermal cycled, and thermal aged) were tested: specimens 19 and 36 from as-built, 3 and 13 from cycling, and specimens 7 and 34 from aging.

The following graphs in Fig.16 illustrate the evolution of crack density as a function of applied mechanical strain during the elevated temperature testing. The graph versus thermo-mechanical transverse stress in 90 layers follows the same trend.

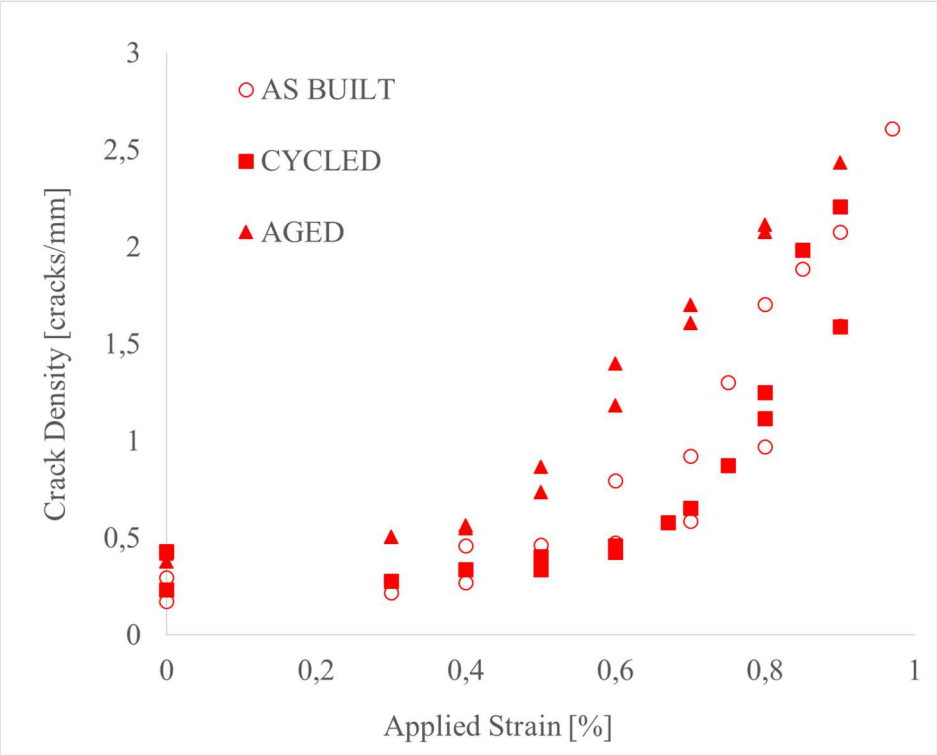

Fig. 16 Crack density evolution vs applied strain during quasi-static tests at elevated temperature (150°C)

Also in this case the damage consists of cracks originating from the threads and propagating into the bundles, or within the bundles only; delamination occurs around 0.7% as well.
As shown in Fig.16, aged specimens display higher damage levels for the same applied mechanical strain, which aligns with previous observations. However, an unexpected result is observed for the cycled specimens in the graph above, where the crack density data points coincide with those of the as-built samples. This is probably due to scatter of data or to errors during the experimental execution of the tests.

Below, in Fig.17, are reported comparative pictures captured by optical microscope for a representative portion of each sample type (as-built, cycled and aged) at a strain level of 0.7%. It can be noticed that, as anticipated by the crack density data, the as-built and cycled specimens exhibit a relatively similar damage in terms of number of cracks, whereas the aged specimens display a more pronounced level of damage.

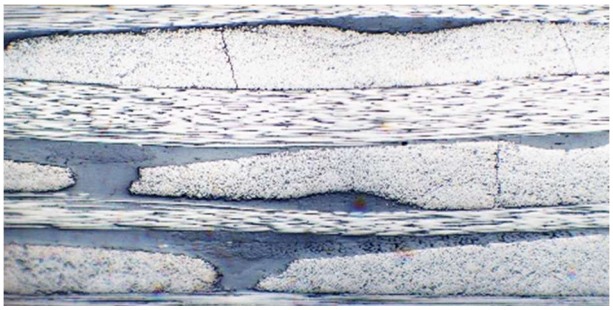

(a)

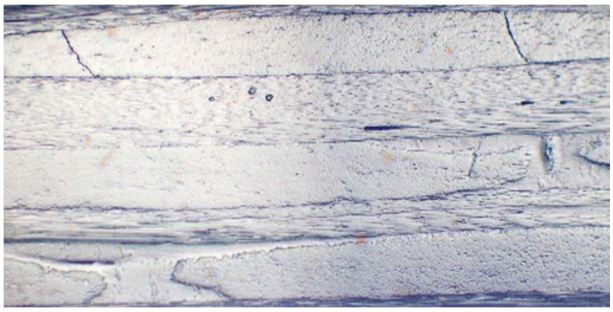

(b)

(c)

Fig. 17 90 layers cracks in (a) as-built, (b) cycled, (c) aged, after 0.7% strain quasi-static tests at elevated temperature

An important analysis to conduct now is the comparison of crack density, considering both applied mechanical strain and thermo-mechanical transverse stress in 90 layer, between the room temperature and elevated temperature tests. Intuitively, a higher damage level was expected in elevated temperature tests; however it was observed the opposite, like shown in the following graphs (Fig.18) of crack density versus applied mechanical strain, for as-built, cycling and aging. In the pictures, the black data-points are referred to quasi-static tests at room temperature and the red data-points to elevated temperature (150°C).

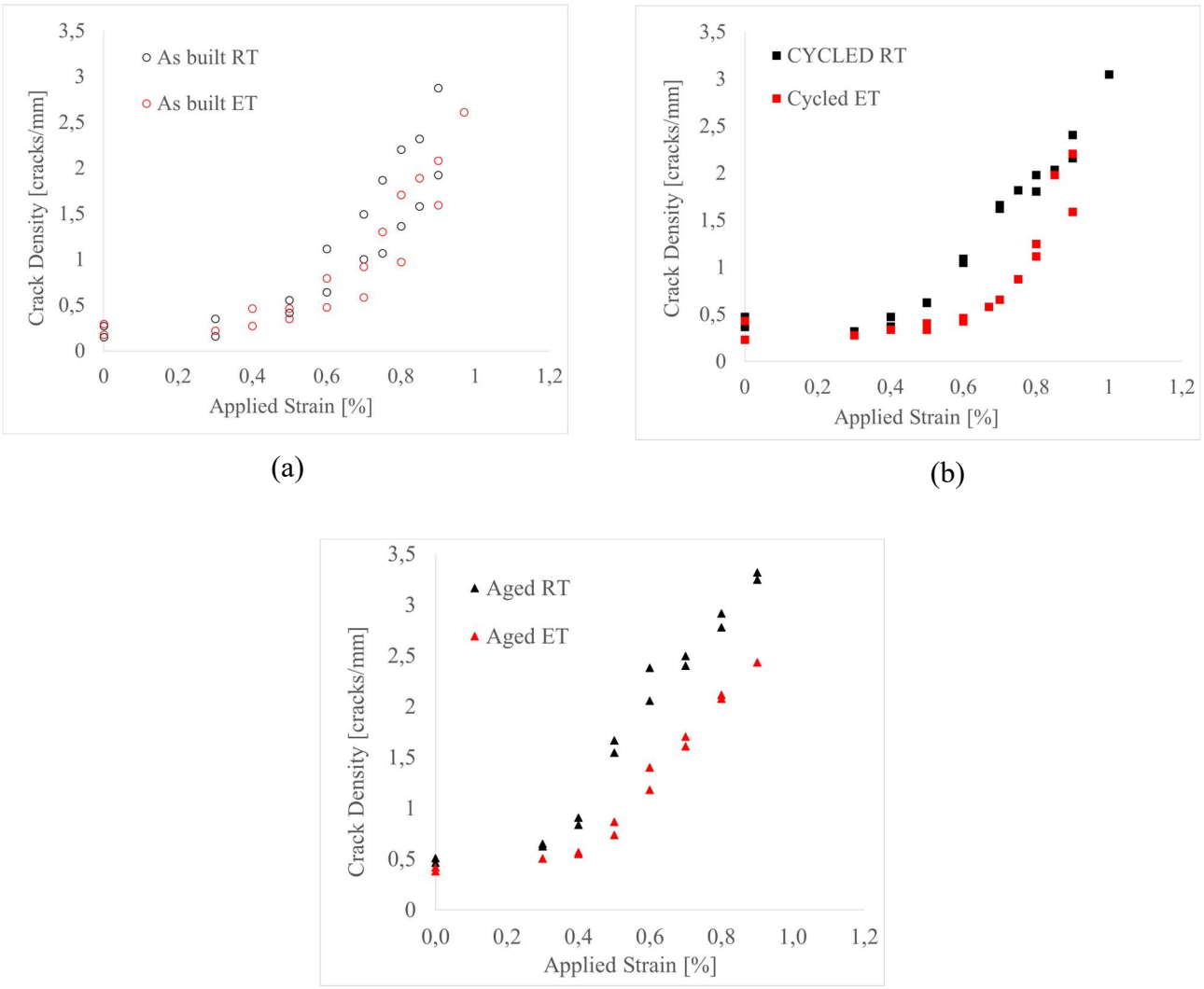

Fig. 18 Crack density vs Applied strain for **(a)** as-built, **(b)** cycling, **(c)** aging. Comparison between room (black) and elevated temperature (red).

The graphs clearly demonstrate that, for the same strain level, the specimens tested at elevated temperature exhibit lower crack density and therefore lower damage. This implies that a higher mechanical strain was required to achieve the same damage level at elevated temperatures, due to the reduced thermo-mechanical transverse stress acting on the 90 layers during testing under elevated temperature conditions.
This effect is shown in the pictures below (Fig.19), comparing samples tested at both room temperature and elevated temperature at the same strain level of 0.7%.

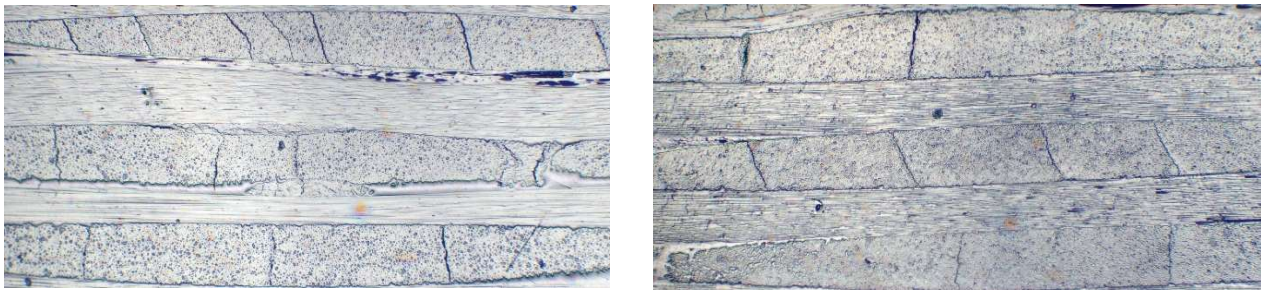

(a) (b)

Fig. 19 Cracks after quasi-static test at 0.7% strain at (a) room T , (b) 150°C

From Fig.19 it is clear that the damage, in terms of number of cracks, at the same strain level of 0.7% is visibly reduced in the samples during the tensile tests conducted at elevated temperatures (b) where the thermo-mechanical transverse stress is lower respect the one conducted at room temperature (a).

This phenomenon is further illustrated in the graph in Fig.20, where crack density is plotted versus the thermo-mechanical transverse stress in 90-layer.
One possible reason why for the same stress level the crack density obtained at elevated temperature is higher than at room temperature could be that the thermo-mechanical transverse stress in 90 layer was determined through Classical Lamination Theory using the UD elastic constants determined at room temperature, since they were not determined yet for 150°C.
Moreover, it can be assumed that when the temperature increases the matrix is subjected to a softening process which degrades the interface bonding strength between the fibers and the matrix, resulting in a significant reduction of the load transfer capacity that the fibers provide to the matrix. Consequently, at 150°C the initial structure of the composite lose rigidity, leading to higher crack density for the same applied thermo-mechanical transverse stress respect to the room temperature [11].

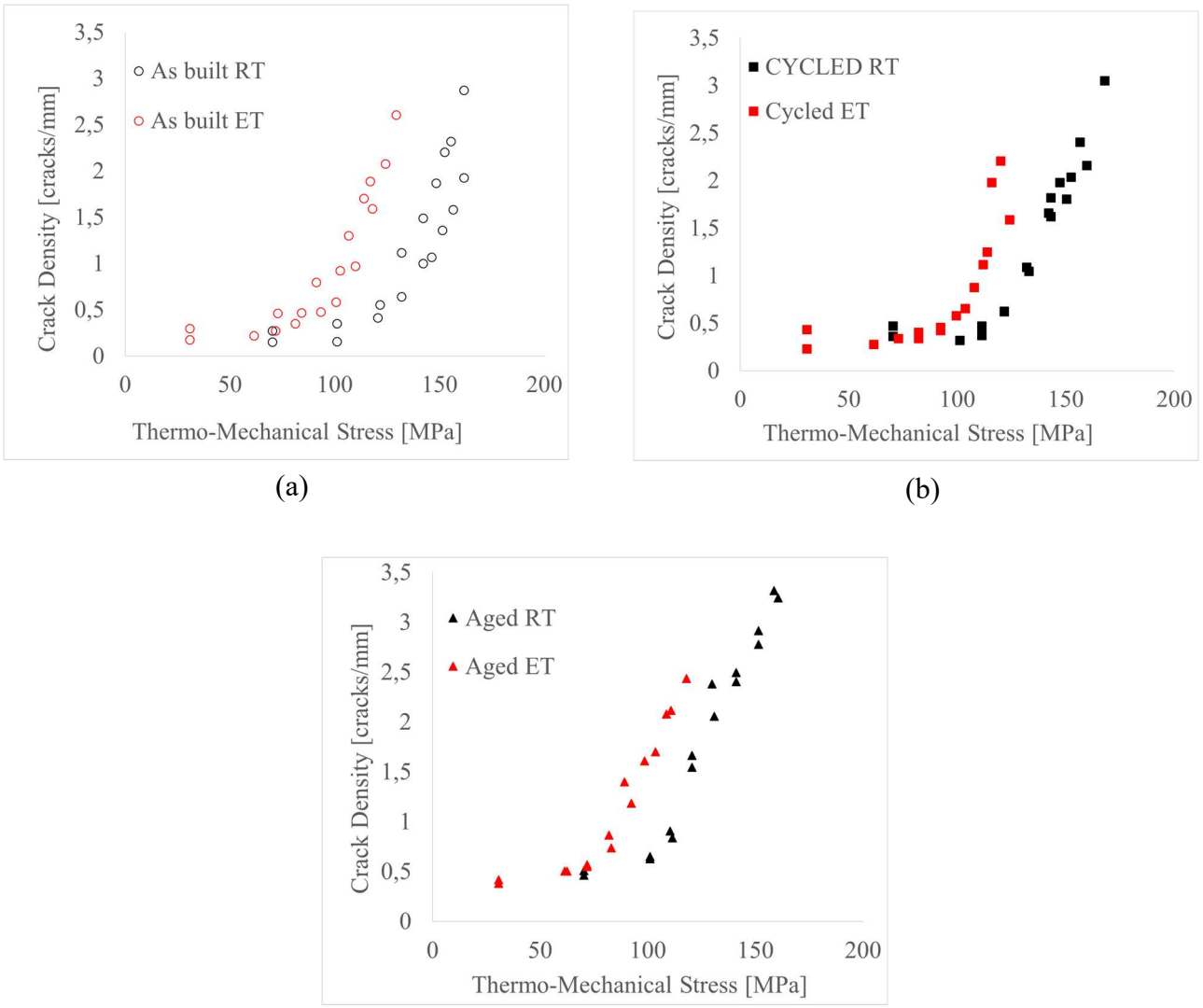

Fig. 20 Crack density vs Thermo-mechanical transverse stress in 90 layers, for (a) as-built, (b) cycling, (c) aging.

Comparison between room (black) and elevated temperature (red)

The following graph (Fig.21) shows the elastic modulus evolution during the quasi-static tests. As it was noticed before, there is some fluctuation in the values, probably due to misalignment of the sample position or the extensometer. However, an overall reduction in the elastic modulus from the initial (before the quasi-static tests) to the final value (after 0.9% strain) can be observed.

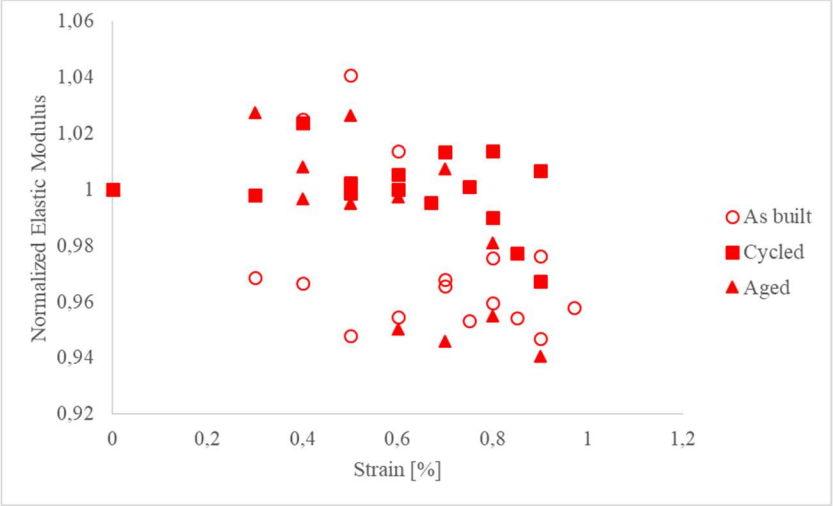

Fig. 21 Normalized elastic modulus evolution versus applied strain during quasi-static tests at elevated temperature

Unexpectedly, Fig.21 reveals a higher reduction in the elastic modulus for the as-built specimens compared to the treated ones. Specifically, the percentage decrement from before and after the quasi-static tests is 5.7% for the as-built specimens, while it is 4.3% and 4.9% for the cycled and aged specimens, respectively. This discrepancy may be attributed again to the misalignment of the extensometer or the behavior of the extensometer itself after exposure to 150 °C. It is possible that the extensometer is not well calibrated immediately after the tests at elevated temperature, as it may still be cooling down.

The following pictures from the microscope (Fig.22) show the delamination occurring at the final stage of the quasi-static tests, specifically at a strain level of 0.9%, for all three specimen types (as-built, cycled and aged) tested at elevated temperatures.
It can be noticed that the degree of local delamination is lower compared to the room temperature tests. Specifically, the pictures reveal that there is minimal or very light delamination in the as-built and cycled specimens. Although the aged samples still exhibit some degree of delamination, it is not as severe as in the room temperature tests. The lower delamination observed at elevated temperatures, similar to the lower crack density, is attributed to the reduced thermo-mechanical transverse stress acting on the 90 layers during testing under elevated temperature conditions.

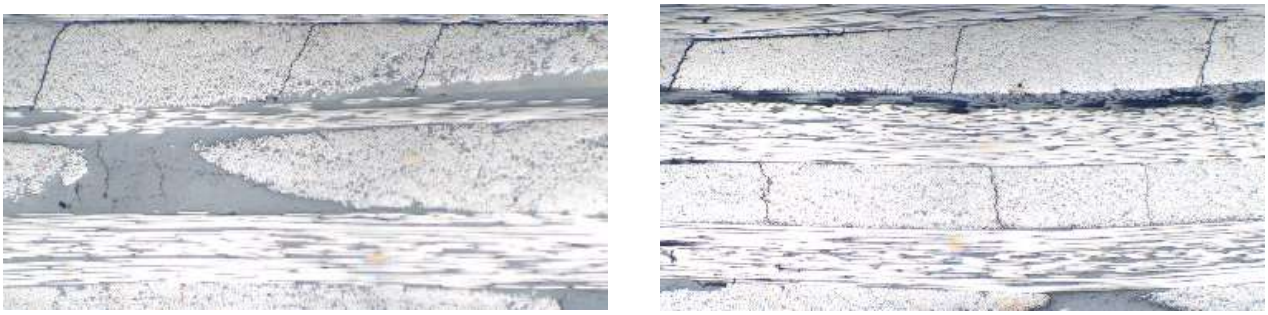

(a) (b)

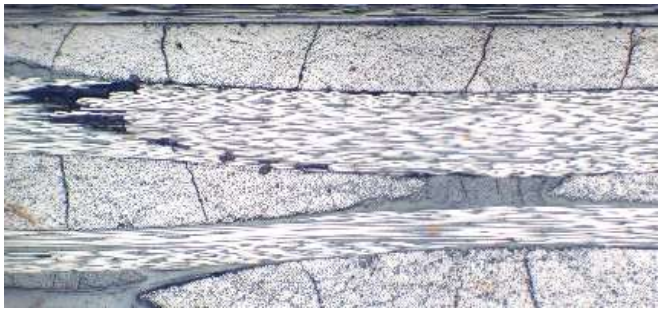

(c)

Fig. 22 Delamination in (a) as-built, (b) cycled, (c) aged, after 0.9% strain quasi-static tests at elevated temperature

Overall, the study has demonstrated the noticeable impact of thermal cycling and thermal aging on the mechanical performance of the material. The treated samples revealed a higher crack density compared to the as-built ones. Although the damage in the thermal cycled specimens was not highly pronounced due to the limited number of cycles, the aging treatment of 1000 hours at 150°C resulted in more significant damage.
Furthermore, the findings show that the thermo-mechanical transverse stress acting on the 90 layers is lower during quasi-static tests performed at elevated temperatures compared to the ones performed at room temperature for the same strain level, resulting in lower damage.
Regarding the elastic modulus, despite the presence of oscillations making the degradation trends unclear, there is a consistent reduction from the initial (before tests) to the final value (after 0.9% strain).

The next step is to develop a prediction model based on the Weibull distribution to forecast the evolution of the crack density in every scenario (as-built elevated temperature, cycled and aged).

3.6 Weibull Prediction Model

With crack density data gathered in the quasi-static tests, a model was developed to predict the data for each condition, including as-built, thermal cycled, and aged specimens, tested at both room and elevated temperatures.
The reference condition for the model are the Weibull parameters σ_0 and m obtained from the as-built specimen tested at room temperature. This configuration was chosen as it is the simplest, most cost-effective, and least time-consuming option to test the material. Once the parameters are obtained, they can be adapted to the more complex conditions, such as thermal treated materials or tests conducted at elevated temperatures.
The procedure for the Weibull parameters calculation was explained in the section 3.5. While only the as-built room temperature parameters are needed as input in the model, the parameters for all other specimens were calculated for comparison purposes and they are reported in the following table.

Tab. 3 Weibull shape and scale parameters for each condition

Specimens condition	Quasi-static test Temperature	Shape parameter m	Scale parameter σ_0
As-built	Room T	5,96	187,8
	150 °C	3,51	168,6
Cycled	Room T	5,37	179,6
	150 °C	4,05	163,5
Aged	Room T	4,29	166,1
	150 °C	2,96	150,8

It is notable that the scale parameters σ_0 for cycled and aged specimens are lower than that of the as-built sample, and they further decrease in tests conducted at elevated temperatures. This decrease can be attributed to the overall reduced inherent strength of the material in these conditions.
The Weibull parameters of the as-built tested at room temperature samples were used as input in the probability of failure prediction formula.

$$P_f = 1 - \exp\left[-\left(\frac{\sigma_T}{\sigma_0}\right)^m\right] \tag{1.1}$$

The corresponding values of thermo-mechanical transverse stress in 90-layer σ_T were obtained through CLT for each scenario (as-built, cycled, aged, room and elevated temperature) and each strain level of quasi-static load.
As example, the obtained probability of failure prediction of an aged specimen is then translated into crack density prediction and plotted together with the experimental data, as shown in the Fig.23 below. The data-points represent the experimental crack density for an

aged specimen, the line represents the crack density prediction using the Weibull parameters from as-built material tested at room temperature.

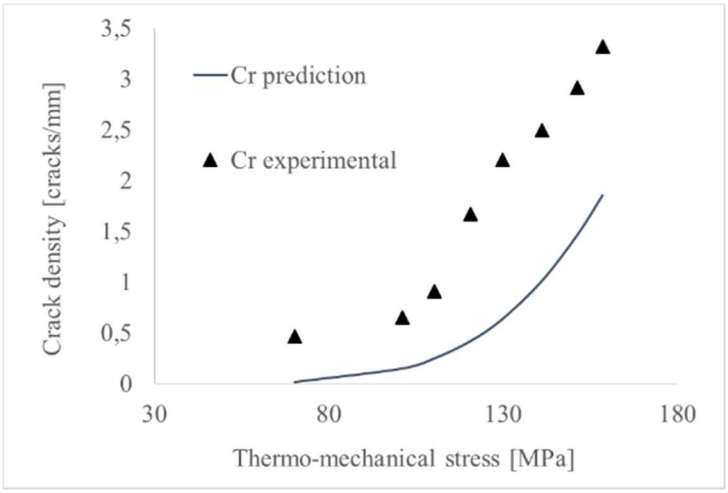

Fig. 23 Comparison between experimental crack density of an aged sample (dots) and predicted crack density (line) using Weibull parameters obtained from as-built room T

It is immediately evident that using only the Weibull parameters from the as-built room temperature sample without any correction yields inaccurate predictions of the crack density, significantly underestimating the crack density of the aged sample. It is obvious that the model requires adaptation to be applicable to other cases, including as-built specimens tested at elevated temperatures, cycled and aged specimens, both at room and elevated temperatures. Specifically, the correction for the scale parameter σ_0 was made, while keeping the shape parameter m fixed. For each thermo-mechanical transverse stress level, the scale parameter in the probability of failure prediction equation was multiplied by a corrective factor k in order to align the prediction curve with each experimental data-point. The individual corrective factors for each strain level were then averaged to obtain a single factor K that, when multiplied by the scale parameter in the equation, ensures a good fit with the experimental data.

$$P_f = 1 - \exp\left[-\left(\frac{\sigma_T}{\sigma_0 \cdot \boldsymbol{K}}\right)^m\right] \tag{1.4}$$

Since these multiplicative factors are function on temperature and sample's conditions, some assumptions were made to give them a plausible physical meaning. In the case of as-built specimens tested at elevated temperatures, the obtained multiplicative factor for the scale parameter is $k = 0.72$, representing the effect of testing at high temperature.

For thermal cycling, it was assumed that the material's degradation and increase in crack density are a function of the number of cycles, thus a decreasing law for the scale parameter depending on the number of cycles was assumed, described by the following equation:

$$\sigma_0 \cdot \boldsymbol{N^{-\alpha}} \tag{1.5}$$

Where *N* represents the number of cycles (15 in this case), and α is an experimental constant, with a value of $\alpha = 0.025$. The experimental constant α is a function of the cycling treatment temperature.

$$\alpha = f(T_{cycling})$$

To account for the effect of testing at elevated temperatures, the equation was further multiplied by the factor $k = 0.72$.
Similarly, for thermal aging, it was assumed that the material's degradation and increase in crack density follow an exponential pattern, as observed in a precedent study, then the degradation law for the scale parameter was assumed and given by the equation

$$\sigma_0 \cdot \boldsymbol{exp(\gamma)} \tag{1.6}$$

Where γ is an experimental constant, with a value $\gamma = -0.2$, it incorporate the aging effect and it is a function of the aging time and temperature.

$$\gamma = f(T_{aging}, t_{aging})$$

Once again, the equation is multiplied by the factor $k = 0.72$ to incorporate the effect of testing at elevated temperatures.
In the table below are summarized the multiplicative factors for each condition.

Tab. 4 Scale parameter correction

Specimens condition	Correction for Room T	Correction for Elevated T (150 °C)
As-built	σ_0	$\sigma_0 \cdot 0.72$
Cycled	$\sigma_0 \cdot N^{-\alpha}$	$\sigma_0 \cdot N^{-\alpha} \cdot 0.72$
Aged	$\sigma_0 \cdot exp(\gamma)$	$\sigma_0 \cdot exp(\gamma) \cdot 0.72$

Using these correction in the formula 1.4 a corrected prediction of the damage for each scenario was obtained, in terms of probability of failure and then translated into crack density.

The following graphs shows a comparison between the experimental crack density data-points and the predicted crack density (line).

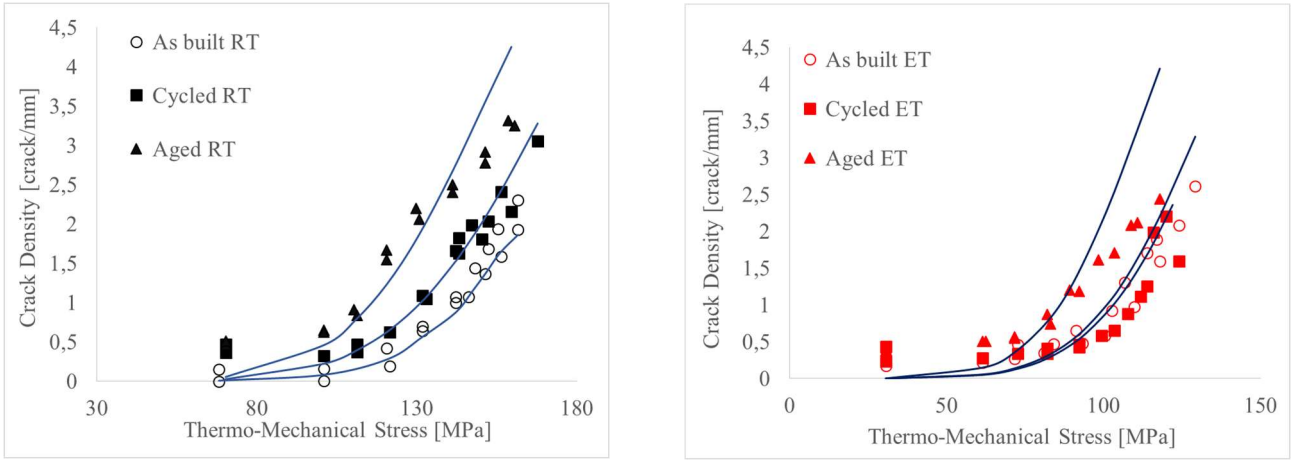

Fig. 24 Fitting of crack density prediction through Weibull model (lines) of experimental crack density (points). For **(a)** room temperature and **(b)** elevated temperature

From the plots it is evident that the introduction of the scale parameter corrections tailored to each case (as-built, cycled and aged) yields a good fit of the crack density prediction (lines) with the experimental data-points, both for quasi-static tests at room temperature (a) and 150°C (b).
However, it can be seen that for aged specimens, the prediction slightly overestimates the experimental data after a certain point. This discrepancy arises because, during the quasi-static tensile testing, the machine reached its loading limit at 0.6% strain, necessitating the grinding of one edge of the samples to reduce the cross-section and continue applying the load without exceeding the machine's limit. However, the elevated temperature exposure during aging affects the surface of the specimen and not the bulk, and by removing the damaged surface through grinding, the effect of thermal aging was eliminated. Consequently, the crack density after grinding was lower than expected. This observation is supported by the lower number of cracks counted after grinding compared to before grinding. In practical applications, where the damaged surface is not removed, a higher experimental crack density would be expected. Therefore, the predictive model still performs well in the case of thermal aging.

For comparison, a similar procedure was conducted to correct the shape parameter m while keeping the scale parameter σ_0 fixed. Although the resulting model also provides reasonable predictions, it was not as accurate as the previous one. Hence, for this study, the focus is on correcting the scale parameter only. Furthermore, there is no justifiable reason to modify the

shape parameter, and it is generally preferable to modify only one parameter while keeping the other fixed.

In conclusion, the crack density prediction model based on Weibull parameters, with specific scale parameter corrections tailored to each thermal treatment (cycling and aging) and for testing at both room and elevated temperatures, demonstrates a good fit with the experimental data. This tool allows for reliable preliminary predictions of the material's behavior, starting from the knowledge of its parameters in as-built condition without requiring expensive and time-consuming testing.

4 Conclusions

In conclusion, this thesis has successfully achieved its aims and objectives of investigating the mechanical behavior of a specific high temperature polymer carbon fiber reinforced composite material under realistic operating conditions , subjecting the material to isothermal cycling and aging to 150°C. The study employed physical characterization techniques, such as optical microscopy, to analyze the material's microstructure and identify changes in crack density and the overall damage state during the cycling and aging and the quasi-static load application.

Quasi-static tensile tests were conducted at both room temperature and elevated temperature of 150 °C on the three sets of as-built, isothermal cycled, and aged specimens.
The results align with theoretical models, demonstrating an increase in crack density increasing the load level. The dominant damage mechanisms involve cracks originating from the threads, propagating within the bundles, and limited to the bundles. Additionally, delamination becomes more prevalent in the later stages of the quasi-static tests. The elastic modulus of the material exhibited a reduction from its initial value before the tests to the final value after 0.9% strain, indicative of mechanical properties degradation.

The effects of thermal cycling and aging on the mechanical performance of the material were significant. An increase in crack density after 15 cycles and 1000 hours of aging was detected. The induced damage of these treatments lead to a lower cracking resistance compared to the as-built samples. While thermal cycling induced moderate damage due to the limited number of cycles, the aging treatment for 1000 hours at 150 °C led to more pronounced damage, including higher delamination and debonding between layers.

Quasi-static tensile tests at elevated temperatures revealed a lower thermo-mechanical transverse stress acting on the 90 layers. Meaning that a lower thermo-mechanical transverse stress level is required to initiate crack propagation at elevated temperatures, thus when the quasi-static load is applied at elevated temperature the material’s cracking resistance is lower.

The development of a statistical prediction model based on the Weibull distribution was a notable achievement of this research. The model, initially established using parameters from the as-built room temperature specimens, was successfully adapted for all other cases through specific corrections of the scale parameter. The predicted crack density aligned well with the experimental data.

This work serves as a preliminary research contribution to the development of a comprehensive damage prediction model for fiber-reinforced composites, it can be concluded that the developed model shows promising performance and is ready for further investigation

5 Acknowledgements

This master thesis "*Study on transverse cracking in aero-engine grade polymer composite under quasi-static loading*" has been carried out at the Materials Science division, Department of Engineering Science and Mathematics of Luleå University of Technology (LTU).

I would like to express my sincere appreciation to the teachers Roberts Joffe and Patrik Fernberg for providing me with the opportunity to work on this project during my thesis.

I am deeply grateful to my supervisor Vivek for his support and guidance and for imparting me his knowledge in the fascinating field of composite materials.

I would also like to acknowledge GKN Aerospace, who provided the project and supplied the necessary materials.

Lastly, thank you to my family, friends and colleagues who have supported me during this journey.

Alessia Cardin

Luleå Tekniska Universitet, June 2023

Bibliography

[1] Aamir, M., Tolouei-Rad, M., Giasin, K., & Nosrati, A. (2019). Recent advances in drilling of carbon fiber–reinforced polymers for aerospace applications: a review. *The International Journal of Advanced Manufacturing Technology*, *105*(5–6), 2289–2308. https://doi.org/10.1007/s00170-019-04348-z

[2] Varna, J., Zrida, H., & Fernberg, P. (2016). Microdamage analysis in thermally aged CF/polyimide laminates. *IOP Conference Series: Materials Science and Engineering*, *139*, 012050. https://doi.org/10.1088/1757-899x/139/1/012050

[3] Richards, P. G. V. (2022). *Transverse Cracking Characterization and Prediction in Heat Treated Polymer Composites under Quasi-Static Tensile Loading at Elevated Temperature*. DIVA. http://ltu.diva-portal.org/smash/record.jsf?dswid=3180&pid=diva2%3A1756797

[4] Zhang, X., Chen, Y., & Hu, J. (2018). Recent advances in the development of aerospace materials. *Progress in Aerospace Sciences*, *97*, 22–34. https://doi.org/10.1016/j.paerosci.2018.01.001

[5] *Polymer Matrix Composites and Technology*. (n.d.). ScienceDirect. https://www.sciencedirect.com/book/9780857092212/polymer-matrix-composites-and-technology

[6] Pimenta, S., & Pinho, S. T. (2011). Recycling carbon fibre reinforced polymers for structural applications: Technology review and market outlook. *Waste Management*, *31*(2), 378–392. https://doi.org/10.1016/j.wasman.2010.09.019

[7] Gabriel, V. R. P., Loukil, M. S., & Varna, J. (2021). Analysis of intralaminar cracking in 90-plies of GF/EP laminates with distributed ply strength. *Journal of Composite Materials*, *55*(26), 3925–3942. https://doi.org/10.1177/00219983211027346

[8] Ben Kahla, H. (2019). Micro-cracking and delaminations of composite laminates under tensile quasi-static and cyclic loading (*PhD dissertation, Luleå tekniska universitet*). Retrieved from http://urn.kb.se/resolve?urn=urn:nbn:se:ltu:diva-73393

[9] Carballal M. M., (2022). Experimental characterization and fatigue damage modelling of aeroengine composites. (*Master thesis*, *Luleå tekniska universitet*)

[10] Mangalgiri, P. (2005). Polymer-matrix Composites for High-temperature Applications. *Defence Science Journal*, *55*(2), 175–193.https://doi.org/10.14429/dsj.55.1980

[11] Li, Q., Gao, Y., & Ruan, F. (2023). The effect of temperature on the tensile properties and failure mechanisms of two-dimensional braided composites. *Science and Engineering of Composite Materials*, *30*(1). https://doi.org/10.1515/secm-2022-0191